 Q. J. R. Meteorol. Soc. 142: 2214–2223, July 2016 A DOI:10.1002/qj.2823

RMetS
Royal Meteorological Society

Laboratory study of a steady-state convective cyclonic vortex

A. Sukhanovskii,* A. Evgrafova and E. Popova
Institute of Continuous Media Mechanics, Perm, Russia

*Correspondence to: A. Sukhanovskii, Laboratory of Physical Hydrodynamics, ICMM, 614013 Perm, Russia. E-mail: san@icmm.ru

An experimental study of the steady-state cyclonic vortex from an isolated heat source in a rotating fluid layer is described. The structure of the laboratory cyclonic vortex is similar to the typical structure of tropical cyclones from observational data and numerical modelling, including secondary flows in the boundary layer. Different constraints of the steady-state hurricane-like vortex were studied. The three main dimensional parameters that define the vortex structure for a fixed geometry – heating flux, rotation rate and viscosity – were varied independently. Characteristics of the steady-state cyclonic vortex were measured experimentally for different values of kinematic viscosity (from 5 to 25 cSt), rotation rate (from 0.04 to 0.17 rad s^{-1}) and heat flux (from 1 to 4.6 kW m^{-2}). The crucial importance for the vortex formation has angular momentum exchange in the viscous boundary layer. It was shown that viscosity is one of the main parameters that define the steady-state vortex structure. Increasing the kinematic viscosity may substantially suppress the cyclonic motion for fixed values of buoyancy flux and rotation rate. Strong competition between buoyancy and rotation provides the optimal ratio of the heating flux and rotation rate for achieving a cyclonic vortex of maximal intensity. It was found that relatively small variation of the rotation rate for the fluids with low kinematic viscosity may remarkably change the cyclonic vortex structure and intensity.

Key Words: rotating layer; cyclonic vortex; localized heat source; convection

Received 6 November 2015; Revised 7 April 2016; Accepted 18 April 2016; Published online in Wiley Online Library 31 May 2016

1. Introduction

Despite decades of research, the problem of tropical cyclogenesis is unsolved and attracts close attention from many scientific groups. The complexity of the problem forces researchers to study tropical cyclogenesis step by step seeing as a main goal the theory that would describe all stages of the tropical cyclone formation. For example, deep convection in tropical depressions, including the effects of boundary-layer wind structure, ambient vertical and horizontal vorticity were studied in a series of idealized numerical experiments (Kilroy and Smith, 2013; Kilroy *et al.*, 2014; Kilroy and Smith, 2015). Laboratory experiments on columnar vortices showed that the formation of an intensive vortex required rotation and some forcing that accumulates extra angular momentum (Morton, 1963; Turner and Lilly, 1963). Rotation has a strong influence on radial inflow which transports additional angular momentum due to centrifugal and Coriolis forces. Recently the rotational constraint on the intensity and size of a tropical cyclone using a minimal, three-layer, axisymmetric tropical cyclone model was studied by Smith and Schmidt (2011). In the first set of numerical experiments, the evolution of a vortex growing from the same initial baroclinic vortex was studied for different values of background rotation characterized by the Coriolis parameter. It was found that the strongest vortices developed in environments with intermediate background rotation and that there exists a similar optimum background rotation strength to obtain the largest storm. The second set of calculations was carried out with a fixed forcing. When the forcing was held fixed, the intensity of the vortex increases monotonically with increasing rotation rate, even for unrealistically large rotation rates. The physical constraints that are necessary for a steady-state tropical cyclone in an isolated environment were studied and discussed by Smith *et al.* (2014). It was pointed out that, without a sufficient source of cyclonic relative angular momentum, the vortex will ultimately decay due to the diffusion of the initial cyclonic angular momentum into the ocean.

There are surprisingly few laboratory experiments considering the formation of intensive cyclonic vortices by convectively driven meridional circulation. A laboratory hurricane model with an analogue of latent heat release was proposed by Hadlock and Hess (1968). They proposed an original approach for the modelling of the latent heat release. At first, a Hadley-like circulation was created by cooling at the periphery of the rotating layer of acid solution. Then, from the holes in the bottom, the base solution was introduced. Chemical reaction between acid and base solutions was exothermic and accompanied by heat release. Resulting vortical flow was similar to the hurricane eyewall. Convection from an isolated source at the bottom for low values of Rossby number with application to the ocean convection was experimentally studied by Brickman and Kelley (1993) and Brickman (1995). These experiments were mainly directed to the study of small eddy formation in a buoyancy source region, their

properties and evolution. Only a short remark was made about the formation of the single cyclonic vortex in the case of high values of convective Rossby number (more than 1). A qualitative experimental study of convective flow driven by a finite-sized circular heating plate at the bottom of a horizontal fluid layer, both with and without background rotation, was carried out by Boubnov and Heijst (1994). In their study the formation of the cyclonic vortex for moderate values of Rossby number ($Ro \approx O(1)$) was also observed, and increasing its intensity with a decreasing rotation rate was mentioned. The studies of Brickman and Kelley (1993), Brickman (1995) and Boubnov and Heijst (1994) showed that, in the case of water ($Pr \approx 7$), cyclonic motion in the lower layer exists only for slow rotation of the vessel.

Another laboratory model of a hurricane-like vortex was proposed and studied by Bogatyrev (1990), Bogatyrev and Smorodin (1996) and Bogatyrev *et al.* (2006). They considered a rotating layer of fluid with a localized heater in the bottom. The important differences of this experimental approach were the use of fluids more viscous than water, and the use of a shallow layer. Local velocity measurements showed that the general structure of mean radial and azimuthal flows in the proposed model is similar to the typical structure of a hurricane. Most of their experiments were carried out with the use of the buoyant probe which indicates only the mean cyclonic motion in a central part. Later, a series of the experiments (Batalov *et al.*, 2010) were done for the same configuration using a particle image velocimetry (PIV) system for velocity measurements. Their main focus was on integral characteristics of the azimuthal flows such as angular momentum and kinetic energy. These studies proved that the experimental configuration of Bogatyrev (1990) is very promising for studying hurricane-like vortices, but many questions concerning the flow structure and its dependence on the key parameters were left open.

Here we focus on the study of different constraints of the steady-state hurricane-like vortex. For a fixed geometry, there are only three main dimensional parameters that define the vortex structure – heating flux, rotation rate and viscosity. All of these parameters are important for the cyclonic vortex formation. The increase of heating flux strengthens secondary circulation and angular momentum transport. The rotation of the layer is the source of intensive vortex formation, but fast rotation may suppress convective motion which would decrease vortex intensity. Viscosity defines angular momentum diffusion and boundary-layer dynamics. So the role of each parameter needs to be studied separately. Another important problem is the choice of non-dimensional parameters; these used for the description of rotating convection depend on several dimensional parameters and sometimes it is unclear which dimensional parameter is more or less important in each particular case. For example, the Grashof number can be varied by heating flux or viscosity or by both of them simultaneously and the way of changing the Grashof number can lead to different flow structures and characteristics. Independently controlled variation of these parameters gives the possibility of analysing the influence of each dimensional parameter on the cyclonic vortex structure and of defining the governing non-dimensional parameters.

The article is organized as follows. In section 2 we describe the experimental set-up and measurement technique. Experimental results are presented in sections 3 and 4. The problem of non-dimensional parameters is discussed in section 5, and conclusions are given in section 6.

2. Experimental set-up

The experimental model is a cylindrical vessel of diameter $D = 300$ mm, and height $H = 40$ mm (Figure 1). The sides and bottom were made of Plexiglas with thicknesses of 3 and 20 mm respectively. There was no cover or additional heat insulation at the sidewalls. The heater is a brass cylindrical plate

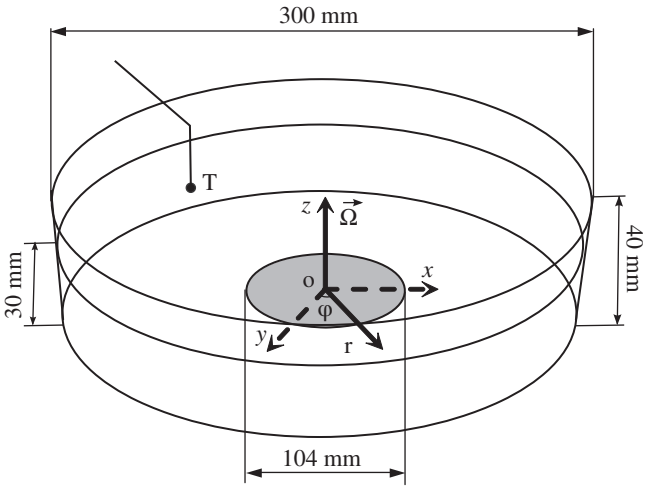

Figure 1. Experimental model, dimensions and location of the coordinate system. T is the thermocouple for control of the mean temperature.

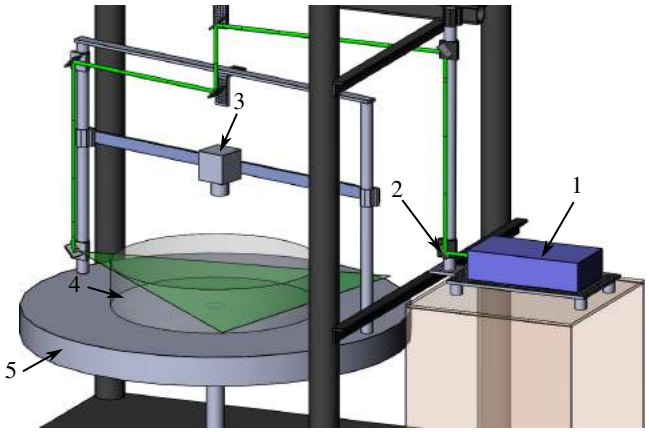

Figure 2. Experimental set-up, showing the dual-pulsed laser for PIV (1), the laser sheet system (2), the CCD camera (3), the experimental model (4), and the rotating table (5).

mounted flush with the bottom. The diameter of the plate d is 104 mm, and its thickness is 10 mm. The brass plate is heated by an electrical coil placed on the lower side of the disc. For studying the influence of the heating on the flow structure, a series of experiments was carried out. For different experimental realizations, the heating power was varied from 8.5 to 39 W. For each realization, the heating power was constant and controlled by a Termodat system. The cylindrical vessel was placed on a rotating horizontal table (Figure 2), which provides uniform rotation in the angular velocity range $0.02 \leq \Omega \leq 0.30$ rad s^{-1} (with accuracy of ± 0.001 rad s^{-1}). In the present study, the angular velocity Ω was varied from 0.04 to 0.17 rad s^{-1}. Silicon oils with different values of kinematic viscosity, PMS-20, PMS-10 and PMS-5 (20, 10 and 5 cSt* at $T = 25\,^{\circ}$C) were used as working fluids. The viscosities of the working fluids were measured at different temperatures by a capillary viscosimeter. In all experiments, the depth of the fluid layer h was 30 mm and the surface of the fluid was always open. The room temperature was kept constant by an air-conditioning system, and cooling of the fluid was provided mainly by the heat exchange with surrounding air on the free surface and some heat losses through sidewalls. For low values of kinematic viscosity, it takes about 2 h to obtain a steady-state regime. Temperature inside the fluid layer was measured at mid-height ($z = 15$ mm), near the periphery (about 3 cm from the sidewall) by a copper-constantan thermocouple. It was used for the estimation of the mean temperature of the fluid. The velocity field measurements were made with a 2D PIV system Polis. The system included a

*centistokes; 1 St = 1 cm^2 s^{-1} = 10^{-4} m^2 s^{-1}.

dual-pulsed Nd-YaG laser, a control unit, a digital charge-couple device (CCD) camera (11 megapixels), placed in a rotating frame, and a computer. The synchronization of the operation of the laser and the CCD camera, the measurement, and the processing of the results were performed using the software package Actual Flow. The cylindrical vessel works as a lens and narrow horizontal light sheet from the periphery to the centre, but all our area of interest in the central part of the vessel was illuminated. Also we need to note that, due to strong optical distortions, we did not make PIV measurements in close proximity to the heater at a height less than 2 mm. All PIV measurements were done for horizontal cross-sections at different heights. Even variation of the three main dimensional parameters (heating, viscosity, rotation) leads to the many experimental realizations (49 in our case). So for the most of experiments, the measurements were done only at three heights, near the bottom ($z = 3$ mm), in the central horizontal cross-section ($z = 15$ mm), and near the upper surface ($z = 27$ mm). This allowed us to study the flow structure in the boundary layer and in the bulk of the flow. For the reconstruction of the mean flow in a vertical cross-section, measurements for several experiments were done in 14 horizontal cross-sections from $z = 2$ to $z = 28$ mm (velocity fields in Figures 6 and 9). Iterative PIV algorithms (Scarano and Riethmuller, 2000) and decreasing of the size of the interrogation windows from 32×32 to 16×16 pixels provided a dynamic range of approximately 500 (the ratio of the maximum and minimum resolvable particle displacement). The PIV velocity measurements were accurate to within 5%, estimated from calibration experiments in solid-body rotation and long time series.

The main subject of this study is a cyclonic vortex over the heating area, so to keep high spatial resolution most of the PIV measurements were made only in a central part of the layer at different horizontal cross-sections. Measurements for several experiments were done for a larger area and with the using of transformer oil as a working fluid (mainly for a description of the general structure of the flow).

Along with the dimensional parameters (heating flux, rotation rate and kinematic viscosity) we use the set of the non-dimensional parameters which are commonly used for similar problems and can help for comparison our results with those obtained by other researchers. These are the flux Grashof number Gr_f, non-dimensional rotation velocity Re, Ekman number E and Prandtl number Pr:

$$Gr_f = \frac{g\beta h^4 q}{c\rho\kappa\nu^2}, \tag{1}$$

$$Re = \frac{\Omega h^2}{\nu}, \tag{2}$$

$$E = \frac{\nu}{\Omega h^2}, \tag{3}$$

$$Pr = \frac{\nu}{\kappa}, \tag{4}$$

where g is the gravitational acceleration, h is the layer depth, β is the coefficient of thermal expansion, c is the thermal capacity, ρ is the density, ν is the coefficient of kinematic viscosity and κ is the thermal diffusivity, q is a heat flux ($q = P/S_h$, P is the power of the heater and S_h is the heater's surface area). The value of non-dimensional rotation velocity Re is equal to the inverse value of Ekman number E, but because of the different physical meaning of these parameters it is convenient to use them both.

3. General structure of the flow

The heat flux in the central part of the bottom initiates the intensive upward motion above the heater. Warm fluid cools at the free surface and moves toward the periphery where the cooled fluid moves downward along the sidewall. After some time, large-scale advective flow occupies the whole vessel (Figure 3, vertical cross-section). Experimental measurements of velocity fields in a non-rotating layer in a vertical cross-section over the heating area showed that instantaneous fields are irregular and asymmetric. Along with the main updraught in the centre, there are less intensive but pronounced upgoing convective flows close to the periphery of the heater (Figure 4).

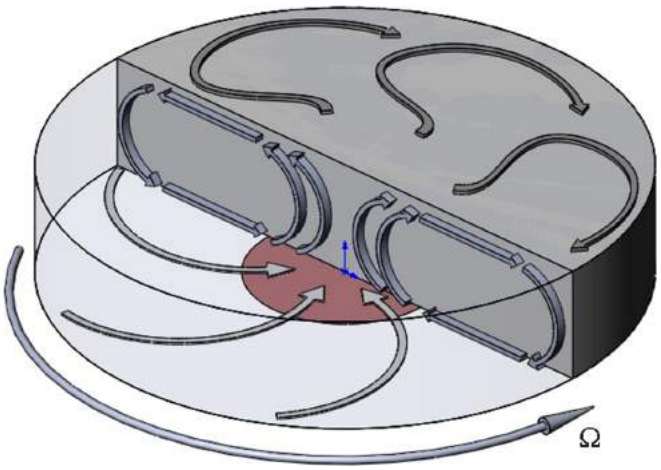

Figure 3. Scheme of the large-scale circulation.

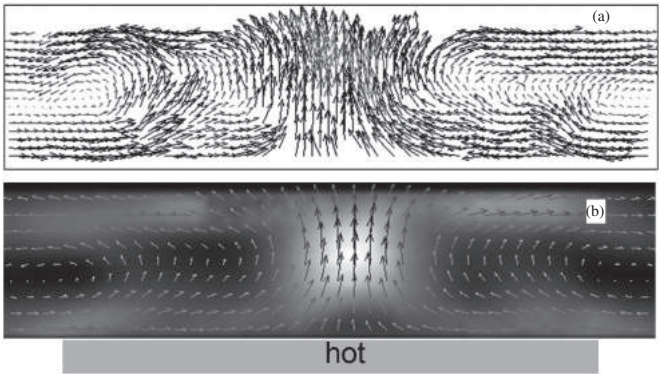

Figure 4. (a) Instantaneous velocity fields in a middle vertical cross-section over the heating area, and (b) mean velocity field in the same cross-section averaged over 190 instantaneous velocity fields (the shaded background shows absolute velocity values). The measurements in a vertical cross-section were done only in a non-rotating layer and mostly for flow visualization because there were evident optical distortions due to the cylindrical shape of the layer.

The large-scale advective flow in the lower part of the layer leads to the formation of boundary layers with potentially unstable temperature stratification above the heater and makes possible the generation of the secondary convective flows (e.g. Batalov *et al.*, 2007; Sukhanovsky *et al.*, 2012). The structure and specifics of secondary flows over the heater in the case of a non-rotating cylindrical layer are described in detail in Sukhanovskii *et al.* (2016). Recent full-scale studies showed that the horizontal rolls are a typical structure of the boundary layer of tropical cyclones and may have a considerable effect on the heat and mass transfer between the water and the air (Morrison *et al.*, 2005; Zhang *et al.*, 2008). We do not concentrate in the current study on the role and influence of the secondary flows on the exchange processes in the boundary layers, since this problem is very complex and deserves special attention.

For illustration of the structure of the secondary flows for high values of Grashof number, we present two shadowgraph images for the same value of Gr_f, with and without background rotation (Figure 5(a, b)). The shadowgraph technique is very efficient for visualization of the small-scale convective structures over the heater. Light rays from a light source located above the experimental model reflect from the surface of the heater and deflect because of temperature disturbances in the boundary layer. (The depth of the boundary layer strongly depends on the kinematic viscosity and varies in our experiments from 3 to

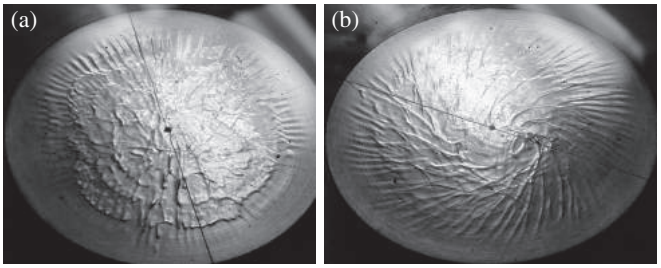

Figure 5. Shadowgraph images of the secondary flows in the thermal boundary layer over the heater. (a) $Gr_f = 1.5 \times 10^7$, $Re = 0$, and (b) $Gr_f = 1.5 \times 10^7$, $Re = 30$.

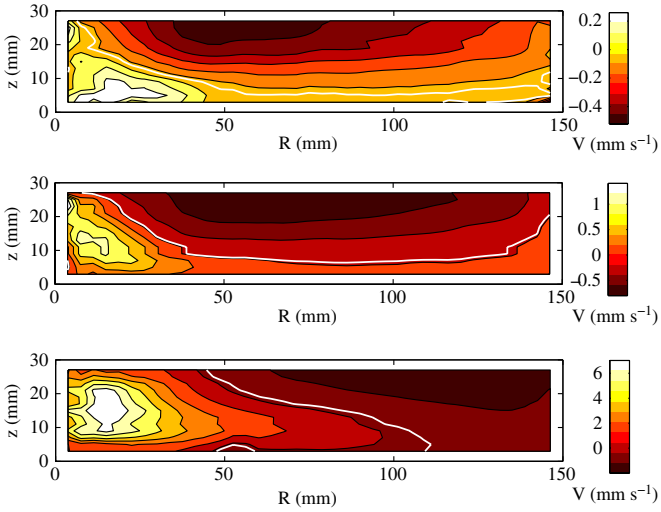

Figure 6. Mean azimuthal velocity fields for (a) $Gr_f = 2.3 \times 10^5$, (b) $Gr_f = 7 \times 10^5$, (c) $Gr_f = 1.5 \times 10^7$, with $\Omega = 0.069\,\mathrm{rad\,s^{-1}}$. Positive values describe cyclonic motion, and negative values anticyclonic motion; the bold white line shows the boundary between cyclonic and anticyclonic flows. Note that, for better representation of the flow structure, the colour scale for each case is different.

7 mm.) The deflections of the light rays produce shadows and make visible areas with high temperature gradients. In the case without background rotation, the structure of the secondary flows is a superposition of radial and transverse rolls (Figure 5(a)). In the rotating layer, convective rolls in the boundary layer are aligned with the large-scale cyclonic flow in the lower layer (Figure 5(b)).

The structure of the steady-state azimuthal flows (in a rotating frame) for different values of Grashof number is shown in Figure 6. Positive (negative) values of velocity describe cyclonic (anticyclonic) motion. Distribution of azimuthal velocity is qualitatively similar to the one of a mature tropical cyclone (Smith *et al.*, 2014). The cyclonic vortex formation in the laboratory system can be described by the following scenario. Large-scale radial circulation leads to the angular momentum transport and angular momentum exchange on the solid boundaries. Convergent flow in the lower layer brings the fluid parcels with large values of angular momentum from the periphery to the centre and produces cyclonic motion (Figure 3, lower horizontal cross-section). In the upper layer the situation is the opposite – divergent flow takes the fluid with low values of angular momentum to the periphery resulting in anticyclonic motion (Figure 3, upper horizontal cross-section). Friction in the viscous boundary layers leads to the sink of angular momentum in the part of the bottom occupied by cyclonic flow and produces source of angular momentum on the sidewalls when anticyclonic flow comes to the periphery. Zero net angular momentum flux on the solid boundaries is the necessary condition for the steady-state regime (Williams, 1968; Read, 1986b; Batalov *et al.*, 2010). Increasing the heating flux produces more intense radial circulation and cyclonic vortex (Figure 6(b, c)) and pushes anticyclonic flow closer to the sidewalls. It is interesting that increasing the heating flux along with the intensification of cyclonic motion decreases integral angular momentum of the layer (Batalov *et al.*, 2010). The strong influence of the sidewalls in a laboratory experiment was noted by Williams (1968) and proved by Read (1986b) and Batalov *et al.* (2010)). If we make sidewalls stress-free, than the necessity of an angular momentum source (to balance the angular momentum sink) leads to the anticyclonic circulation in the peripheral part of the bottom and stronger decrease of integral angular momentum of the layer than in the case of solid-body rotation.

Hadley-like circulation in the rotating layer produces azimuthal flows and there is a need for a theory to describe this processes. A theoretical approach for the description of the flow in a rotating layer with horizontal temperature gradient was developed by Hignett *et al.* (1981) and Read (1986b), where parameter Q (the ratio between depths of the thermal and Ekman boundary layers) was introduced as a governing parameter. This theory has a good qualitative agreement with experimental studies (Hignett *et al.*, 1981) for a rotating layer of low viscous fluid (water or paraffin, $Pr = 7$ and $Pr = 16$ respectively), and for low values of Ekman number ($E < 10^{-3}$). The attempt to use the same approach in the different case of viscous fluids ($Pr > 63$) and relatively slow rotation ($E > 0.03$), carried out by Batalov *et al.* (2010) and Sukhanovsky (2011), showed that parameter Q cannot be used for the flow description. It means that there is a requirement for a new theoretical approach which will help to describe the formation of azimuthal flows in a rotating layer with horizontal temperature gradient for the case when the thickness of the viscous boundary layer is not negligibly small in comparison with the depth of the layer. The main question in relation to the cyclonic vortex formation in a described statement of the problem is how to predict the structure and intensity of the vortex for the prescribed initial and boundary conditions and physical properties of the working fluid.

4. Dependence of the cyclonic vortex structure on the main parameters

This section presents results of three sets of experiments. Our purpose here is to describe the flow structure and its evolution with variation of one of the main parameters. We chose nine experiments (Table 1) which clearly illustrate the role of each parameter. First, we vary the heating power while keeping the rotation rate and viscosity (approximately) constant (Experiments 1–4; Figure 7). Second, we vary the viscosity while keeping the rotation rate and heating power constant (Experiments 3, 5, 6; Figure 8). Finally, we vary the rotation rate while keeping the heating power and viscosity constant (Experiments 4, 7, 8; Figure 9).

4.1. *Variation of heating*

Relative motion of the fluid is driven by localized heating so a clear understanding of how the increase of the heating changes the flow structure is very important. The structure of the mean steady-state azimuthal flows (in a rotating frame) for different values of Grashof number which characterizes the ratio of the buoyancy and viscous forces is shown in Figure 6. The presented azimuthal velocity fields were obtained for the transformer oil as a working fluid. Transformer oil has strong dependence of viscosity on temperature, so the result of the remarkable growth of the cyclonic vortex intensity comes from the simultaneous variation of two main parameters – heating and viscosity. In order to minimize the effect of the decreasing viscosity with the temperature variation, we have made a series of measurements using silicon oils. Their physical properties are significantly less dependent on temperature than is transformer oil. Variation of values of kinematic viscosity for the following series of experiments was less than 20%.

Spatially and time-averaged radial and azimuthal velocity profiles for different heating power and for three heights, near

Table 1. The values of the main parameters.

Experiment	P (W)	Ω (rad s^{-1})	ν (cSt)	Gr_f	Re	E	Pr	Fluid
1	8.5	0.08	5.6	2.6×10^6	13.2	0.076	63	PMS-5
2	13.5	0.08	5.3	4.1×10^6	13.7	0.073	60	PMS-5
3	19	0.08	5.1	6.0×10^6	14.7	0.068	57	PMS-5
4	39	0.08	4.7	1.4×10^7	15.6	0.064	53	PMS-5
5	19	0.08	21	2.7×10^5	3.4	0.29	215	PMS-20
6	19	0.08	9	1.5×10^6	8.3	0.12	97	PMS-10
7	39	0.11	4.7	1.4×10^7	21.3	0.047	53	PMS-5
8	39	0.17	4.7	1.4×10^7	32.3	0.031	53	PMS-5
9	19	0.17	5.1	6.0×10^6	30.6	0.033	57	PMS-5

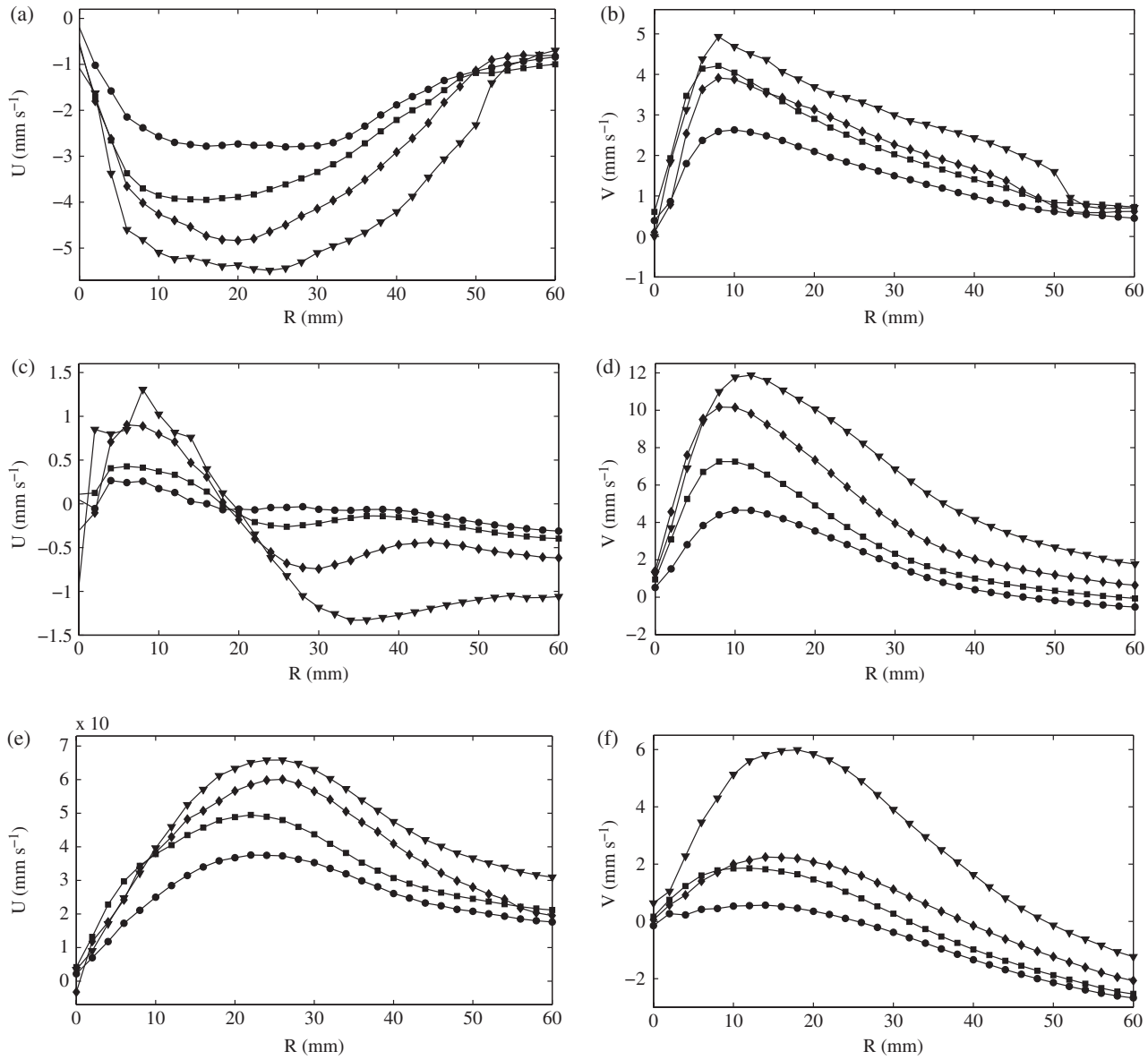

Figure 7. Mean radial (a,c,e) and azimuthal (b,d,f) velocity profiles for three heights: (a, b) 3 mm, (c, d) 15 mm, and (e, f) 27 mm, for different heating in experiments (listed in Table 1) 1 (circles), 2 (squares), 3 (diamonds), and 4 (triangles). The rotation rate is fixed, variation of viscosity with heating is less than 20%.

the bottom ($z = 3$ mm), in the middle of the layer ($z = 15$ mm) and near the upper boundary ($z = 27$ mm) for the one working fluid (PMS-5) are presented in Figure 7. The values of the main parameters for experiments in Figure 7 are shown in Table 1. This series of measurements characterized by small variation of viscosity which does not lead to the substantial change of non-dimensional rotation rate Re or Ekman number E (which defines the depth of the viscous boundary layer). It is expected that the increase of the heating would produce more intensive meridional circulation and the presented results confirm this (Figure 7(a, e)). The magnitude of radial velocity U near the bottom is less than near the free surface due to the non-slip condition on the bottom. Also the radial velocity in the middle of the layer changes its direction (Figure 7(c)). The mean radial velocity field in the vertical cross-section (Figure 9(a)) illustrates the structure of radial velocity for experiment 4. It shows that convergent and divergent radial flows are not symmetrical and the boundary between them is not horizontal. We did not present velocity profiles for fluids with higher values of kinematic viscosity because the main influence of the increase of ν on the meridional circulation is the decrease of its intensity due to viscous friction.

The meridional circulation provides angular momentum transport in the lower layer and the magnitude of azimuthal velocity depends on the intensity of convergent flow (Figure 7(b)).

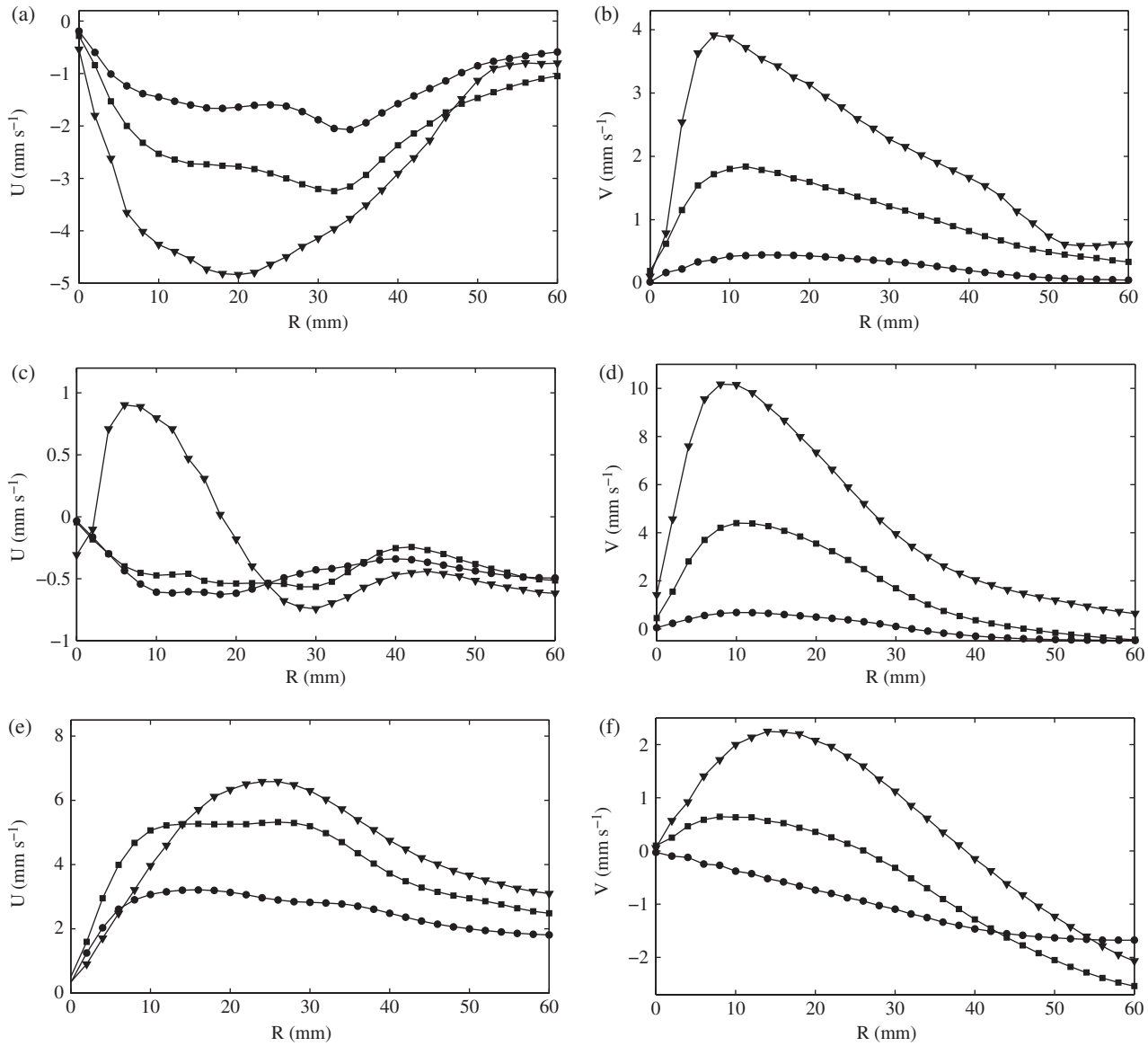

Figure 8. Mean radial (a,c,e) and azimuthal (b,d,f) velocity profiles for three heights: (a, b) 3 mm, (c, d) 15 mm, and (e, f) 27 mm for different values of viscosity in experiments 6 (circles), 5 (squares), and 3 (triangles). Heating and rotation rates are fixed.

The magnitude of azimuthal velocity V above in the middle and upper layer also increases with the heating. Profiles of V in the upper layer (Figure 7(f)) show that the structure of the cyclonic vortex changes with heating; it becomes more uniform over depth. The shape of the vortex is conical for weak heating and becomes cylindrical (in the central part) in the developed state (Figures 6 and 9(b)). The general structure of both radial and azimuthal velocity fields presented in Figure 9(a, b) are similar to the observational data from Zhang *et al.* (2011b).

4.2. *Variation of viscosity*

Another important parameter that has crucial importance on the cyclonic vortex formation is viscosity. In order to separate effects of viscosity, we have made three series of measurements for fluids with substantially different values of kinematic viscosity for fixed values of heat flux and rotation rate. It means that we consider the rotating layer of fluid with constant energy source and study what would happen with the cyclonic vortex with variation of the physical properties of the fluid. Velocity profiles for $P = 19$ W are shown in Figure 8, and values of the main parameters for experiments 3, 5, 6 are presented in Table 1. High viscosity strongly decreases angular momentum transport because viscous friction in the thick boundary layer effectively damps excessive angular momentum when a fluid parcel moves to the centre. As a result, we have a very weak cyclonic vortex in the central part of the lower layer and anticyclonic flow which occupies most of the fluid layer similar to Figure 6(a). Decrease of kinematic viscosity leads to the remarkable increase of cyclonic vortex intensity. We believe that this result might be very important because spatial or time dependence of turbulent viscosity in the atmospheric flows may lead to strong variation in the magnitude of the wind velocity and spatial inhomogeneity of temperature and velocity fields.

4.3. *Variation of rotation*

The third parameter studied is the rotation rate. In our case the rotation is the source of angular momentum so the faster we rotate the layer, the more intense is the vortex potentially produced. On the other hand, rotation suppresses convection which is the main source of the meridional circulation which brings extra angular momentum to the centre and produces a cyclonic vortex. This means that, for a fixed rotation rate, increasing the heating leads to increase of the cyclonic vortex intensity. (We do not consider extreme values of the heating when large-scale radial circulation becomes unstable.) However, for fixed heating, there is an optimal rotation rate which provides the most intensive cyclonic vortex. The existence of the optimal rotation rate in a laboratory experiment was found by Bogatyrev and Smorodin (1996), where measurements were carried out using a buoyant probe which showed angular velocity of the cyclonic vortex averaged over depth. The buoyant probe was a very efficient tool

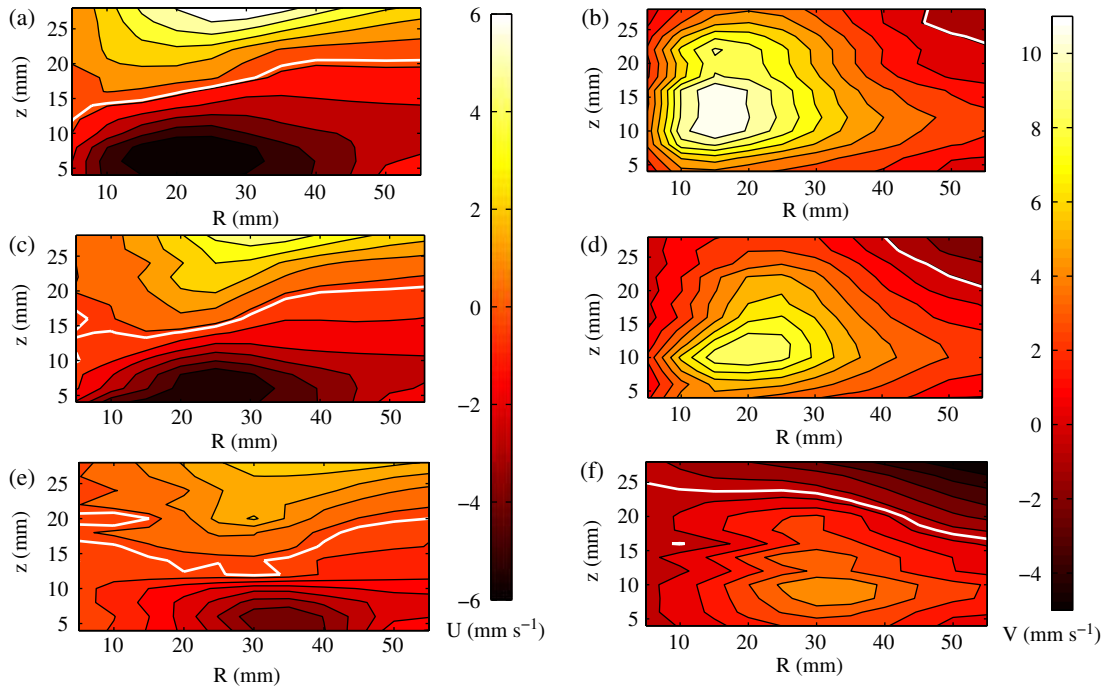

Figure 9. Mean (a, c, e) radial and (b, d, f) azimuthal velocity fields for three experiments (a, b) 4, (c, d) 7, and (e, f) 8. Positive values denote cyclonic motion, negative values anticyclonic motion, and the bold white line shows the boundary between cyclonic and anticyclonic flows.

for the qualitative study of the cyclonic vortex but, for studying the flow structure, a non-invasive technique such as PIV is required. Figure 9 presents mean velocity fields in a vertical cross-section for fixed heating and different rotation rates (experiments 4, 7, 8). There is a remarkable change of the flow structure with a relatively small variation of the rotation rate (from 0.17 to 0.08 rad s^{-1}). The meridional circulation produced by localized heating has the shape of a toroidal cell. When rotation is relatively slow and has weak influence on convective flows, the convective toroidal cell occupies almost the whole layer. Increasing the rotation rate moves the convective cell from the centre and decreases its intensity. Radial velocity fields (Figure 9(a, c, e)) show that the maximum radial velocity is shifted to the periphery for higher rotation rates and its magnitude decreases. The azimuthal velocity fields show strong correlation between the structure of the meridional circulation and the cyclonic vortex (Figure 9(b, d, f)). The vertical velocity distribution is also very important because radial flow delivers additional angular momentum to the central part of the lower layer and then upgoing flows transport angular momentum further to the middle and upper layers. We did not measure the vertical component of velocity, but for non-divergent flow radial and vertical components of velocity are linked, so the structure of the vertical velocity field also strongly depends on the rotation rate and the maximum vertical velocity moves from the centre with an increase in rotation rate. In this case we have convective updraught flows in the ring area at some distance from the centre instead of intensive upgoing jet as in Figure 4. In Figure 10 we present mean vector fields at $z = 3$ mm for experiments 3 and 9 which are both at lower Grashof number but differ only in rotation rate. This shows that, with increase of rotation rate, a concentrated cyclonic vortex becomes a vortical ring.

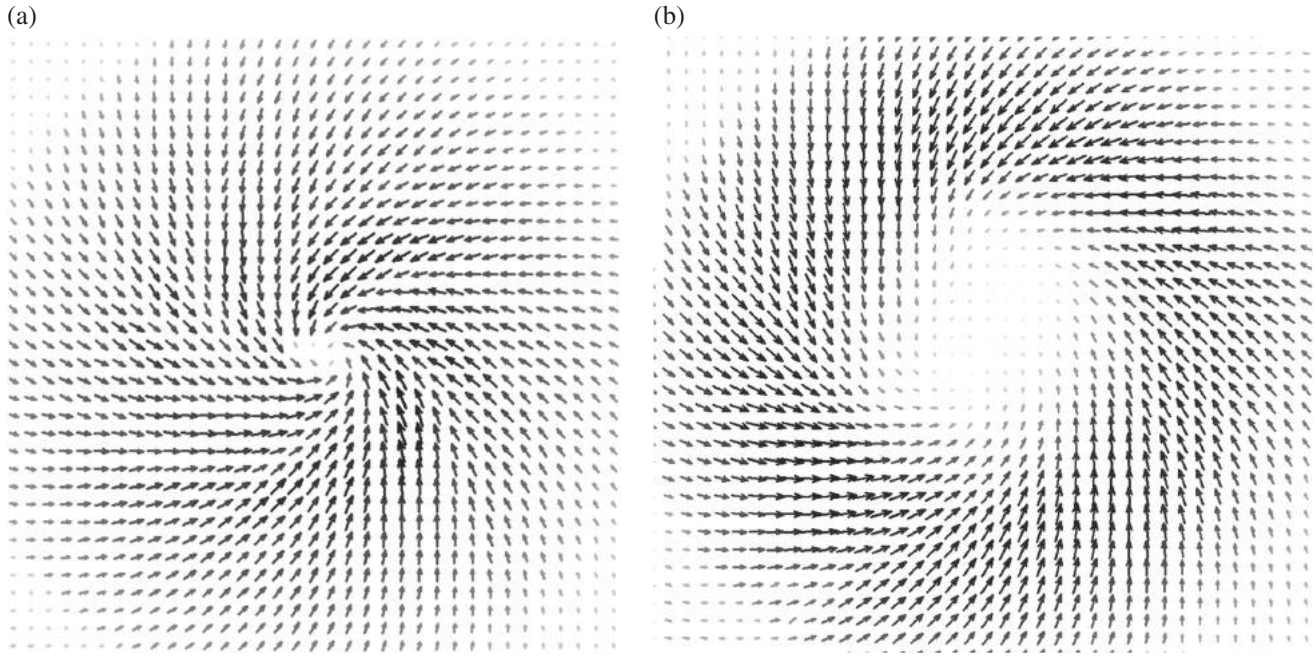

Figure 10. Mean vector velocity fields for $z = 3$ mm, $Gr_f = 6 \times 10^6$, $Pr = 57$: (a) $Re = 14.7$ (experiment 3), and (b) $Re = 30.6$ (experiment 9).

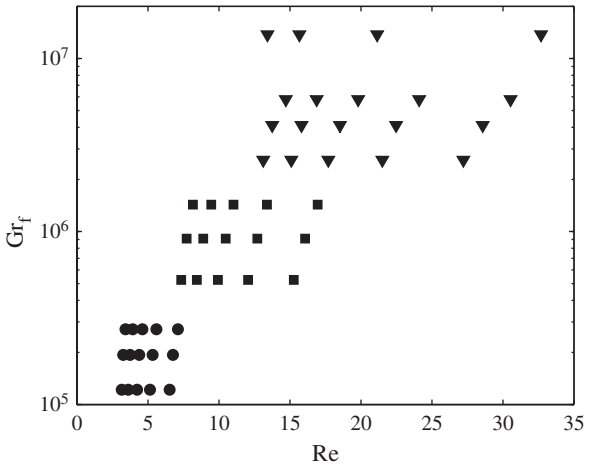

Figure 11. All experiments in the plane $Gr_f - Re$, using PMS-20 (circles), PMS-10 (squares), and PMS-5 (triangles).

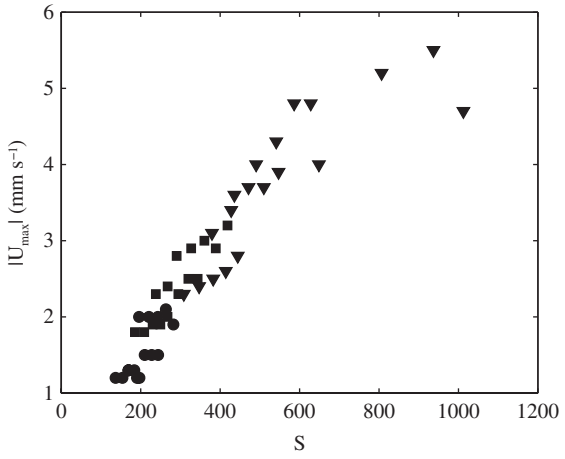

Figure 12. Maximal magnitude of radial velocity U_{max} versus S at $z = 3$ mm, using PMS-20 (circles), PMS-10 (squares), and PMS-5 (triangles).

5. Non-dimensional parameters

An important issue is the combination of non-dimensional parameters that defines the structure and characteristics of the cyclonic vortex in a steady-state regime. We mentioned earlier that, usually for laboratory study of vortical flows, water ($Pr = 7$ at $T = 20\,^{\circ}$C) is used as a working fluid. Experiments with water for small values of Ekman number were quite efficiently described by convective Rossby number which does not depend on viscosity (Brickman and Kelley, 1993; Maxworthy and Narimousa, 1994; Brickman, 1995). We showed that in our case viscosity and viscous boundary layers are crucial for cyclonic vortex formation so convective Rossby number cannot be chosen as a governing parameter. The meridional circulation in our experiments has a convective nature and for a fixed rotation rate is defined by the Grashof number (Batalov *et al.*, 2010), the depth of the viscous boundary layer depends on Ekman number, and the rotation is characterized by non-dimensional rotation rate, so we have made the attempt to find the dependence of the flow characteristics on a combination of these non-dimensional parameters. Systematic measurements were done for the three different values of the heating power (8.5, 13.5, 19 W), the five rotation rates (0.08, 0.094, 0.11, 0.134, 0.17 rad s^{-1}) and for the three different fluids (PMS-5, PMS-10 and PMS-20), altogether 45 experiments. Additionally we carried out four experiments for the low viscous fluid (PMS-5) and higher heating power (39 W) for different rotation rates (0.07, 0.08, 0.11, 0.17 rad s^{-1}). Figure 11 shows all 49 experiments in the plane $Gr_f - Re$; because of the strong influence of viscosity, the experiments for different working fluids are marked by different symbols. In the present study the velocity measurements were done only in the central part of the vessel so we cannot use the integral characteristics such as energy of radial or azimuthal motions for description of the flow as in Batalov *et al.* (2010). Instead the maximal values of radial and azimuthal velocity were chosen for analysis as the flow characteristics. We have tried different non-dimensional combinations and finally came to conclusion that the best choice for the governing parameter is the square root of the ratio of Grashof number and non-dimensional rotation rate (Eq. (5)). The parameter S is proportional to the product of characteristic spin-up time t_s (Greenspan, 1968) and the square root of the heat flux:

$$S = \sqrt{\frac{Gr_f}{Re}} \;\propto\; t_s\sqrt{q}, \qquad t_s = \frac{h}{\sqrt{\nu\Omega}}. \tag{5}$$

The maximum of absolute value of radial velocity U increases with S (Figure 12). This means that the intensity of the radial flow increases with the heating and decreases with the rotation rate and viscosity. For high values of Prandtl number (PMS-20, $Pr > 200$) the rotation is not a primary parameter and convection dominates. With decreasing Prandtl number, the role of the rotation becomes more and more important. The formation of azimuthal flows in the lower layer essentially depends on the rotation rate and the radial convergent flow. Figure 13 shows that the ratio of magnitudes of maximal radial and azimuthal velocity decreases with increase of non-dimensional rotation rate and Grashof number. This decrease is very fast for the small values of $(Gr_f Re)$ and then it varies slightly around unity. The behaviour of the flow in the middle layer is more complex because of competiton between rotation, which suppresses vertical motions, and buoyancy. For characterization of azimuthal flow in the middle layer, we choose non-dimensional relative azimuthal velocity $V_{max,rel}$ which is the ratio of maximal azimuthal velocity V_{max} to the azimuthal velocity of solid-body rotation at the same radius R_{max}:

$$V_{max,rel} = \frac{V_{max}}{\Omega \times R_{max}}. \tag{6}$$

We mentioned earlier that there is optimal rotation rate for the fixed heating power when the cyclonic vortex becomes most intensive. Summarizing data from all our experiments, we see that $V_{max,rel}$ is defined by the non-dimensional parameter S and there is indeed an optimal ratio of the heating and rotation for cyclonic vortex formation (Figure 14). An increase of S leads to the growth of $V_{max,rel}$ up to some value of S, and then further increase of S decreases $V_{max,rel}$. There are some experiments that do not fit the described dependence of V_{max} on S. They are marked as open triangles and represent experiments for low viscous fluid (PMS-5) and fast rotation rates ($Re > 22$) when the structure of the cyclonic flow is changed from the localized vortex to the vortical ring. The variation of V_{max} with Re for the same working fluid but different heating power is similar. To show this, we separated all experimental data on four groups for different values of the heating power (8.5, 13.5, 19 and 39 W), then we normalized maximal azimuthal velocities (at $z = 15$ mm) for each group by highest value of V_{max} for the corresponding value of the heating power, P. The result is presented in Figure 15. It is clearly seen that dependencies of normalized values of V_{max} on the non-dimensional rotation rate are similar for the same working fluid and different values of the heating power. Low viscous fluids show strong dependence on the rotation rate for all values of the heating power, and high viscous fluids are almost independent of the rotation rate.

6. Conclusions

The structure of the laboratory cyclonic vortex is similar to the typical structure of tropical cyclones from observational data and numerical modelling, including secondary flows in the boundary

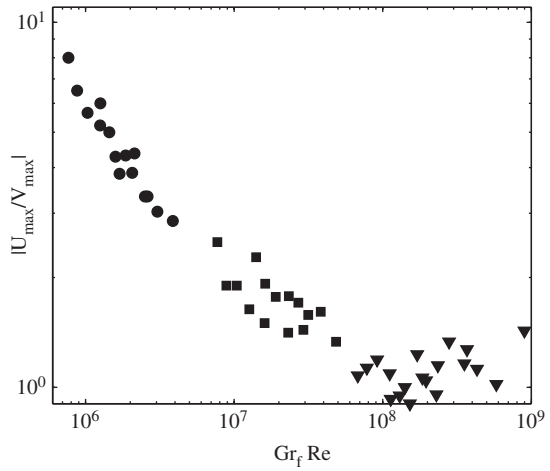

Figure 13. Log–log plot of ratio of maximal magnitude of radial velocity U_{max} to maximal magnitude of azimuthal velocity V_{max} versus $Gr_f Re$ at $z = 3$ mm, using PMS-20 (circles), PMS-10 (squares), and PMS-5 (triangles).

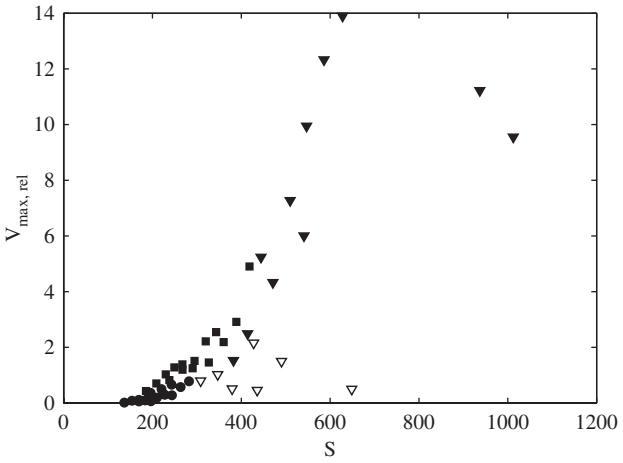

Figure 14. Relative maximal azimuthal velocity $V_{max,rel}$ versus S at $z = 15$ mm, using PMS-20 (circles), PMS-10 (squares), PMS-5 (solid triangles), and PMS-5 with $\Omega > 0.13$ (open triangles).

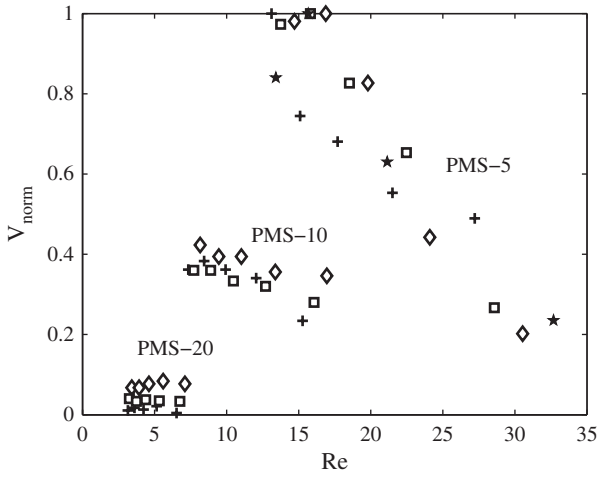

Figure 15. Normalized values of V_{max} versus Re at $z = 15$ mm, for $P = 8.5$ W (crosses), 13.5 W (open squares), 19 W (open diamonds), and 39 W (stars).

layer. Laboratory modelling reproduces some of the essential features of the tropical cyclone and may serve as a very useful tool for analysing the influence of different parameters on tropical cyclone formation. The role of the three main parameters of the problem – heating, rotation and viscosity – was studied separately. Independent controlled variation of these parameters gives us the possibility of analysing the influence of each dimensional parameter on the cyclonic vortex structure and of defining governing non-dimensional parameters.

The first parameter is the heating which is the driving source of the fluid motion. Increase of the heating power in the chosen range of parameters always leads to an increase of the cyclonic vortex intensity. The structure of the cyclonic vortex changes with the heating and becomes more uniform over the depth. The shape of the vortex is conical for weak heating and becomes cylindrical (in the central part) in the developed state.

Another important parameter that has crucial importance on the cyclonic vortex formation is viscosity. In order to separate effects of viscosity, we have made three series of measurements for fluids with substantially different values of kinematic viscosity for fixed values of heat flux and rotation rate. High viscosity strongly decreases angular momentum transport because viscous friction in the thick boundary layer effectively damps all excessive angular momentum when a fluid parcel moves to the centre. As a result there is a very weak cyclonic vortex in the central part of the lower layer and anticyclonic flow that occupies most of the fluid layer. Decreasing of kinematic viscosity leads to a remarkable increase of cyclonic vortex intensity. We assume that this result might be very important because spatial or time dependence of turbulent viscosity in atmospheric flows may lead to a strong variation of the magnitude of the wind velocity and spatial inhomogeneity of temperature and velocity fields.

The third parameter is the rotation rate. Rotation is the source of angular momentum, so the faster we rotate the layer, the more intensive the vortex may appear. On the other hand, rotation suppresses convection which is the main source of the meridional circulation which brings extra angular momentum to the centre and produces the cyclonic vortex. As a result of competition between convection and rotation, there is an optimal value of the non-dimensional complex S which provides the most intensive cyclonic vortex. Experiments with a low viscous fluid (PMS-5) and fast rotation rates ($Re > 22$) do not fit the described dependence of relative azimuthal velocity on S and show a qualitative change of the flow structure with increasing rotation rate. The convective cell is pushed from the centre and the concentrated cyclonic vortex becomes the vortical ring. Finally we want to emphasize our main result that relatively small variations of viscosity and rotation rate may remarkably change the cyclonic vortex structure and its intensity.

Acknowledgements

We sincerely thank Peter Frick and the anonymous referees for constructive comments which led to serious improvement of the article. The financial support of grants RFBR No.14-01-96011 and No.16-31-00150 is gratefully acknowledged.

References

Batalov VG, Sukhanovskii AN, Frick PG. 2007. Experimental investigation of helicoidal rolls in an advective flow over a hot horizontal surface. *Fluid Dyn.* **42**: 540–549.

Batalov V, Sukhanovskii A, Frick P. 2010. Laboratory study of differential rotation in a convective rotating layer. *Geophys. Astrophys. Fluid Dyn.* **104**: 349–368.

Bogatyrev GP. 1990. Excitation of a cyclonic vortex or a laboratory model for a tropical cyclone. *Pisma Zh. Eksp. Teor. Fiz.* **51**: 557–559.

Bogatyrev GP, Smorodin BL. 1996. Physical model of the rotation of a tropical cyclone. *Pisma Zh. Eksp. Teor. Fiz.* **63**: 25–28.

Bogatyrev GP, Kolesnichenko IV, Levina GV, Sukhanovsky AN. 2006. Laboratory model of generation of a large-scale spiral vortex in a convectively unstable rotating fluid. *Izv. Atmos. Oceanic Phys.* **42**: 423–429.

Boubnov BM, van Heijst GJF. 1994. Experiments on convection from a horizontal plate with and without background rotation. *Exp. Fluids* **16**: 155–164.

Brickman D. 1995. Heat flux partitioning in open-ocean convection. *J. Phys. Oceanogr.* **25**: 2609–2623.

Brickman D, Kelley DE.1993. Development of convection in a rotating fluid: Scales and pattern of motion. *Dyn. Atmos. Oceans* **19**: 389–405.

Greenspan HP. 1968. *The Theory of Rotating Fluids*. Cambridge University Press: New York, NY.

Hadlock RK, Hess SL. 1968. A laboratory hurricane model incorporating an analog to release of latent heat. *J. Atmos. Sci.* **25**: 161–177.

Hignett P, Ibbetson A, Killworth PD. 1981. On rotating thermal convection driven by non-uniform heating from below. *J. Fluid Mech.* **109**: 161–187.

Kilroy G, Smith RK. 2013. A numerical study of rotating convection during tropical cyclogenesis. *Q. J. R. Meteorol. Soc.* **139**: 1255–1269.

Kilroy G, Smith RK. 2015. Tropical cyclone convection: The effects of a vortex boundary-layer wind profile on deep convection. *Q. J. R. Meteorol. Soc.* **141**: 714–726.

Kilroy G, Smith RK, Wissmeier U. 2014. Tropical convection: The effects of ambient vertical and horizontal vorticity. *Q. J. R. Meteorol. Soc.* **140**: 1756–1770.

Maxworthy T, Narimousa S. 1994. Unsteady, turbulent convection into a homogeneous, rotating fluid, with oceanographic applications. *J. Phys. Oceanogr.* **24**: 865–887.

Morrison I, Businger S, Marks F, Dodge P, Businger JA. 2005. An observational case for the prevalence of roll vortices in the hurricane boundary layer. *J. Atmos. Sci.* **62**: 2662–2673.

Morton BR. 1963. Model experiments for vortex columns in the atmosphere. *Nature* **197**: 840–842.

Read PL. 1986. Super-rotation and diffusion of axial angular momentum: II. A review of quasi-axisymmetric models of planetary atmospheres. *Q. J. R. Meteorol. Soc.* **112**: 253–272.

Scarano F, Riethmuller ML. 2000. Advances in iterative multigrid PIV image processing. *Exp. Fluids* **29**: S051–S060.

Smith RK, Schmidt CW. 2011. An investigation of rotational influences on tropical-cyclone size and intensity. *Q. J. R. Meteorol. Soc.* **137**: 1841–1855.

Smith RK, Montgomery MT, Persing J. 2014. On steady-state tropical cyclones. *Q. J. R. Meteorol. Soc.* **140**: 2638–2649.

Sukhanovsky AN. 2011. Formation of differential rotation in a cylindrical fluid layer. *J. Fluid Dyn.* **46**: 158–168.

Sukhanovsky A, Batalov V, Teymurazov A, Frick P. 2012. Horizontal rolls in convective flow above a partially heated surface. *Europ. Phys. J. B* **85**: 9, doi: 10.1140/epjb/e2011-20420-7.

Sukhanovskii A, Evgrafova A, Popova E. 2016. Horizontal rolls over localized heat source in a cylindrical layer. *Physica D* **316**: 23–33.

Turner JS, Lilly DK. 1963. The carbonated-water tornado vortex. *J. Atmos. Sci.* **20**: 468–471.

Williams GP. 1968. Thermal convection in a rotating fluid annulus: Part 3. Suppression of the frictional constraint on lateral boundaries. *J. Atmos. Sci.* **25**: 1034–1045.

Zhang JA, Katsaros KB, Black PG, Lehner S, French JR, Drennan WM. 2008. Effects of roll vortices on turbulent fluxes in the hurricane boundary layer. *Boundary-Layer Meteorol.* **128**: 173–189.

Zhang JA, Rogers RF, Nolan DS, Marks FD Jr. 2011. On the characteristic height scales of the hurricane boundary layer. *Mon. Weather Rev.* **139**: 2523–2535.

